

Elastic-Differential Cross Section of $\pi^+ + p$ at 1.5, 2.0, and 2.5 BeV/c*

VICTOR COOK, BRUCE CORK, AND WILLIAM R. HOLLEY

Lawrence Radiation Laboratory, University of California, Berkeley, California

AND

MARTIN L. PERL

University of Michigan, Ann Arbor, Michigan

(Received 7 November 1962)

We measured elastic-scattering angular distributions for $\pi^+ + p$ scattering at 1.5, 2.0, and 2.5 BeV/c using spark chambers to detect scattered pions and protons. A bump that decreases in amplitude with increasing momentum is observed in the backward hemisphere in the 1.5- and 2.0-BeV/c distributions, but is not observed in the 2.5-BeV/c distributions. It appears reasonable to attribute this phenomenon to the 1.45-BeV/c resonance observed in the $\pi^+ + p$ total cross section. The data are compared with $\pi^- + p$ data and are found to support the theoretical prediction that the scattering cross sections for both charge states should become equal at high energies. We fit the angular distributions with a power series in $\cos\theta^*$, and compare the extrapolated values for the scattering cross section in the backward direction with the calculation of the neutron-exchange pole contribution to the cross section. The "elementary" neutron-pole term contribution is calculated to be 90 mb/sr at 2.0 BeV/c, in violent disagreement with the extrapolated value, ≈ 0.5 mb/sr.

I. INTRODUCTION

THE elastic-differential cross sections of positive pions on protons at incident-pion momenta of 1.5, 2.0, and 2.5 BeV/c have been measured for pion-scattering angles greater than about 9 deg in the laboratory system. The existing evidence concerning the pion-nucleon interaction at high energy can be summarized as follows:

At about 1.5 BeV/c, the $\pi^+ + p$ total cross section appears to have a broad resonance, whereas from 2 BeV/c upward the variation of the total cross section with energy is smooth and slowly decreasing.^{1,2} Our lowest momentum measurement coincides with the highest momentum $\pi^+ + p$ resonance known. For convenience, we shall refer to the entire region below 2 BeV/c as the "resonance region" of pion-nucleon interactions.

The behavior of the $\pi^+ + p$ and $\pi^- + p$ total cross sections from 2.5 BeV/c upward can be described as an approach to an asymptotic high-energy limit. At that high-energy limit the behavior is predicted to be very simple³; the total cross sections for $\pi^+ + p$ and $\pi^- + p$ should approach the same value; the elastic total and differential cross sections should also become equal; and the charge-exchange cross section should go to zero. Additionally, recent dispersion theories⁴ lead to specific conjectures about the behavior of the differential-elastic

cross section with energy for the low momentum-transfer (diffraction-scattering) region.

The purpose of our measurements was to extend the known $\pi^+ + p$ elastic-differential cross section from the resonance region to the beginning of the asymptotic region. Three things will be discussed specifically: first, the effect of the 1.45-BeV/c $\pi^+ + p$ total cross-section "resonance" on $\pi^+ + p$ and $\pi^- + p$ elastic scattering; second, the degree to which the $\pi^+ + p$ and $\pi^- + p$ elastic cross sections become similar as the incident-pion momentum increases; third, the evidence of a peak in the backward-scattering region.

II. EXPERIMENTAL METHOD AND RESULTS

The measurement was carried out at the Bevatron during an extensive experiment on K^+ interactions by Cook *et al.*⁵ During the time that the Bevatron beam was being used primarily for another experiment, the K^+ -beam apparatus was tuned for π^+ . About 5% of the internal proton beam provided sufficient π^+ flux for this experiment. Since the equipment used was the same as in the K^+ experiment and is discussed in detail elsewhere,⁵ only a very brief description is given here. The apparatus, Fig. 1, consisted of a 4-ft-long hydrogen target surrounded on the front and sides in the horizontal plane by three spark chambers which were in turn surrounded by an array of scintillation counters. The chambers were pulsed when the counters indicated an interaction had occurred with at least two roughly coplanar outgoing particles. The three spark chambers, each with a 90-deg stereo view, were photographed on a single film frame.

All of the film was scanned at the Lawrence Radiation Laboratory and separately scanned at the University of Michigan. We selected elastic events by requiring that the events be coplanar within 3 deg and that the

* Supported in part by the Office of Naval Research and by the U. S. Atomic Energy Commission.

¹ T. J. Devlin, B. C. Barish, W. N. Hess, V. Perez-Mendez, and J. Solomon, *Phys. Rev. Letters* **4**, 242 (1960).

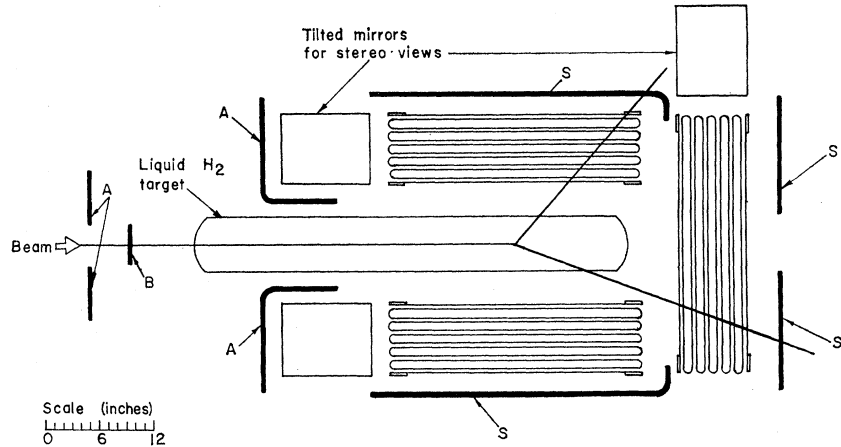
² M. J. Longo, J. A. Helland, W. N. Hess, B. J. Moyer, and V. Perez-Mendez, *Phys. Rev. Letters* **3**, 568 (1959); G. von Dardel, D. Dekkers, R. Mermod, M. Vivargent, G. Weber, and K. Winter, *ibid.* **8**, 173 (1962); S. J. Lindenbaum, W. A. Love, J. A. Niederer, S. Ozaki, J. J. Russell, and L. C. L. Yuan, *ibid.* **7**, 352 (1961).

³ I. Ya. Pomeranchuk, *Soviet Phys.—JETP* **7**, 499 (1958); V. S. Barashenkov, *Soviet Phys.—Usp.* **3**, 689 (1961).

⁴ V. Singh and B. M. Udgaonkar, *Phys. Rev.* **123**, 1487 (1961).

⁵ V. Cook, D. Keefe, L. T. Kerth, P. G. Murphy, W. A. Wenzel, and T. F. Zipf, *Phys. Rev.* **129**, 2743 (1963).

FIG. 1. Horizontal section of the apparatus. The heavy lines represent scintillation counters. Those labeled *S* are the spark chamber trigger counters; *A* indicates anticounters; *B* is the target defining counter. A typical scattering event is indicated schematically.



angles of the proton and pion differ no more than 4 deg from the kinematic prediction. Actually 80% of all events accepted as elastic were coplanar within 2 deg and agreed with the kinematic prediction within two degrees. The total number of pictures taken was about 25 000, of which 3307 were finally accepted as elastic. We corrected the data for geometric bias introduced by the counters, scanning bias, beam attenuation in the hydrogen target, absorption of the scattered proton, loss of elastic events by nuclear and multiple scattering, contamination by inelastic events from the hydrogen, and μ^+ and e^+ contamination in the beam.

The results are given in Figs. 2, 3, and 4. The θ^* is the angle of the scattered pion in the barycentric system. Statistical errors and uncertainties in corrections contribute approximately equal amounts to the total $\pi^+ + p$ errors. In addition to the errors shown, there is an over-all uncertainty of $\pm 15\%$ in the absolute

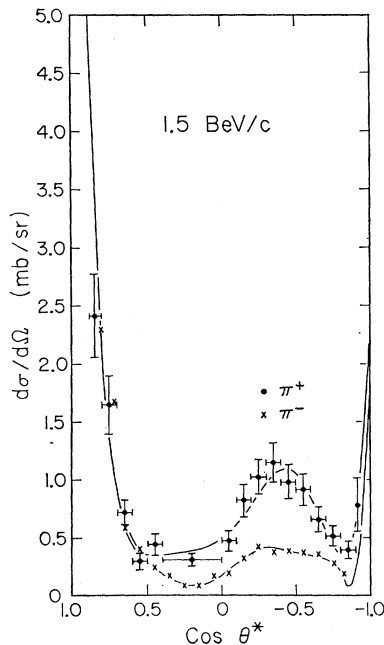


FIG. 2. Elastic-differential cross section at 1.5 BeV/c for $\pi^+ + p$ and $\pi^- + p$ (forward point from reference 9; other data from reference 8) in the barycentric system against the angle of the scattered pion in that system. The backward peak at $\cos\theta = -1$ in the $\pi^- + p$ cross section is a result of the fitting procedure.

normalization due largely to uncertainties in μ^+ and e^+ contamination. To simplify the comparison with $\pi^- + p$, the corresponding $\pi^- + p$ differential cross section⁶⁻⁸ are also shown. The errors on the π^- points are not shown but are about the same size as the π^+ errors. Normalization uncertainties are about the same for both π^+ and π^- .

The data are also presented in Tables I, II, and III. In the calculation of the values of $d\sigma/d\Omega$ at 0 deg, we derived the imaginary part of the forward-scattering amplitude from the total cross sections given in reference 2. The real part of the forward-scattering ampli-

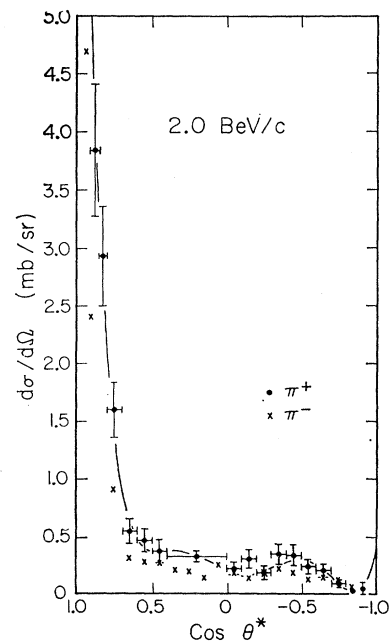


FIG. 3. Elastic-differential cross section at 2.0 BeV/c for $\pi^+ + p$ and $\pi^- + p$ (two most forward points from reference 10; other data from reference 8) in the barycentric system against the angle of the scattered pion in that system.

⁶ K. W. Lai, L. W. Jones, and M. L. Perl, Phys. Rev. Letters 7, 125 (1961).

⁷ M. Chretien, J. Leitner, N. P. Samios, M. Schwartz, and J. Steinberger, Phys. Rev. 108, 383 (1957).

⁸ V. Cook, B. Cork, T. F. Hoang, D. Keefe, L. T. Kerth, W. A. Wenzel, and T. F. Zipf, Phys. Rev. 123, 320 (1961).

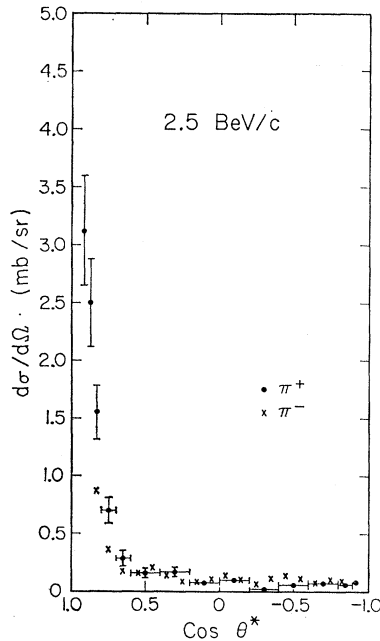


FIG. 4. Elastic-differential cross section at 2.5 BeV/c for $\pi^+ + p$ and $\pi^- + p$ (from reference 8) in the barycentric system against the angle of the scattered pion in that system.

tude was taken from the calculation of Cronin,⁹ except that his assumption of constant behavior of the total cross section at very high energy was replaced by the asymptotic behavior of the total cross section given in reference 2. The total elastic scattering cross sections for π^+ and π^- are given in Table IV.

The $\pi^+ - p$ and $\pi^- - p$ ⁶ distributions have been fitted with a power series in $(\cos\theta^*)^n$. At 2.5 BeV/c, both distributions require at least 10th or 11th order terms, and the same is true of the $\pi^- - p$ data at 2.0 BeV/c. The best values for the power-series coefficients for the 1.5- and 2.0-BeV/c data are given in Table V, and the cross sections calculated from these coefficients are plotted in Figs. 2 and 3.

III. DISCUSSION

First, we consider the comparison of the $\pi^+ + p$ and $\pi^- + p$ differential cross sections at 1.5 BeV/c. The diffraction peaks are quite similar, but the $\pi^+ + p$ has a large backward "bump" (to be distinguished from backward "peak" which refers to the peak at

TABLE I. Elastic-differential cross section for $\pi^+ + p$ scattering at 1.5-BeV/c incident- π momentum.

$\cos\theta^*$	$d\sigma/d\Omega$ (mb/sr)	$\cos\theta^*$	$d\sigma/d\Omega$ (mb/sr)
1.00	12.7 ± 1.24	-0.25	1.02 ± 0.15
0.838	2.42 ± 0.36	-0.35	1.14 ± 0.17
0.75	1.65 ± 0.25	-0.45	0.98 ± 0.15
0.55	0.30 ± 0.07	-0.55	0.91 ± 0.14
0.45	0.44 ± 0.09	-0.65	0.66 ± 0.11
0.2	0.31 ± 0.05	-0.75	0.51 ± 0.09
-0.05	0.47 ± 0.09	-0.85	0.39 ± 0.08
-0.15	0.82 ± 0.14	-0.915	0.78 ± 0.23

⁹ J. W. Cronin, Phys. Rev. **118**, 824 (1960).

TABLE II. Elastic-differential cross section for $\pi^+ + p$ scattering at 2.0-BeV/c incident- π momentum.

$\cos\theta^*$	$d\sigma/d\Omega$ (mb/sr)	$\cos\theta^*$	$d\sigma/d\Omega$ (mb/sr)
1.00	10.4 ± 0.96	-0.15	0.31 ± 0.08
0.882	3.84 ± 0.57	-0.25	0.19 ± 0.06
0.825	2.93 ± 0.44	-0.35	0.35 ± 0.09
0.75	1.60 ± 0.24	-0.45	0.34 ± 0.09
0.65	0.54 ± 0.11	-0.55	0.24 ± 0.06
0.55	0.47 ± 0.10	-0.65	0.21 ± 0.05
0.45	0.37 ± 0.09	-0.75	0.10 ± 0.03
0.2	0.33 ± 0.05	-0.85	0.03 ± 0.02
-0.05	0.22 ± 0.06	-0.915	0.05 ± 0.05

$\cos\theta^* = -1$) which reaches a maximum of 1.1 mb/sr at about $\cos\theta^* = -0.5$, whereas the $\pi^- + p$ only reaches about 0.3 mb/sr. Thus, the effect of the isotopic spin-3/2 "resonance," which appears at 1.45 BeV/c in the $\pi^+ + p$ total cross section, may also be evident in the $\pi^+ + p$ elastic cross section and, to a lesser extent, also in the $\pi^- + p$ elastic cross section.

At 2.0 BeV/c the $\pi^+ + p$ cross section is still greater than the $\pi^- + p$ cross section; the total elastic cross section is about 25% greater; and in the region outside of the forward scattering peak, from $\cos\theta^* = +0.2$ to $\cos\theta^* = -1.0$, the average differential cross section is

TABLE III. Elastic-differential cross section for $\pi^+ + p$ scattering at 2.5-BeV/c incident- π momentum.

$\cos\theta^*$	$d\sigma/d\Omega$ (mb/sr)	$\cos\theta^*$	$d\sigma/d\Omega$ (mb/sr)
1.00	13.9 ± 1.4	0.10	0.08 ± 0.02
0.916	3.12 ± 0.47	-0.10	0.10 ± 0.03
0.87	2.50 ± 0.38	-0.30	0.02 ± 0.01
0.825	1.55 ± 0.23	-0.50	0.06 ± 0.02
0.75	0.70 ± 0.11	-0.70	0.07 ± 0.02
0.65	0.29 ± 0.06	-0.85	0.06 ± 0.02
0.50	0.16 ± 0.04	-0.925	0.09 ± 0.05
0.30	0.17 ± 0.04		

0.21 ± 0.035 mb/sr for $\pi^+ + p$ compared to 0.16 ± 0.025 mb/sr for $\pi^- + p$. However, at 2.5 BeV/c the total elastic and differential-elastic cross sections are the same within the errors of this experiment.

Thus, although 2.5 BeV/c is only the beginning of the asymptotic region, the elastic-differential cross sections are already the same within the errors of these experiments, namely, within about 25%. Thus, this experiment supports the general picture that for increasing incident-pion momenta above the region of pion-proton resonances, not only are the total pion-proton cross sections becoming independent of the pion charge, but

TABLE IV. Total elastic scattering cross sections in mb.

P_{π}^{lab} (BeV/c)	$\pi^+ + p$	$\pi^- + p$
1.5	13.8 ± 2.0	10.4 ± 1.5
2.0	10.6 ± 1.5	8.0 ± 1.5
2.5	6.9 ± 1.0	7.3 ± 1.1

TABLE V. Best values found for coefficients of $\cos\theta$ power-series fits to the $\pi^+ - p$ and $\pi^- - p$ elastic-scattering angular distributions.

	$\pi^+ - p$		$\pi^- - p$
P_{π}^{lab} (BeV/c)	1.5	2.0	1.5
Order of best fit	6	6	7
$P(x^2)$	0.16	0.60	0.48
F^a	0.16	0.14	0.75
a_0	0.47 ± 0.07	0.22 ± 0.03	0.15 ± 0.02
a_1	-1.03 ± 0.31	0.52 ± 0.16	-0.09 ± 0.13
a_2	3.37 ± 0.93	1.41 ± 0.46	1.15 ± 0.36
a_3	-0.12 ± 1.42	-3.79 ± 0.79	2.36 ± 1.24
a_4	-13.97 ± 3.05	-6.18 ± 1.53	-5.99 ± 1.31
a_5	5.55 ± 1.52	7.97 ± 0.92	-9.42 ± 3.37
a_6	16.69 ± 2.67	9.68 ± 1.36	8.75 ± 1.25
a_7			12.23 ± 2.64

^a Probability that next highest term is zero, calculated using the Fisher "F" test.

the elastic-differential cross sections are also becoming independent of the pion charge.

Finally, we consider the possibility of a backward peak in the differential cross section. We observe that the power-series fits to the $\pi^+ + p$ angular distributions at 1.5 and 2.0 BeV/c indicate the presence of a peak at $\cos\theta^* = -1$ in both of these distributions.¹⁰ We must point out, however, that we have no data in the crucial region between $\cos\theta^* = -0.95$ and -1.0 . Thus we depend upon extrapolated curves which indicate the presence of considerable structure in the backward region. This is particularly noticeable in the curve fitted to the data at 1.5 BeV/c shown in Fig. 2. There were no measurements made beyond $\cos\theta^* = -0.85$ for this process, so the backward peak is a result of the fitting procedure. (The peak is much smaller in the next highest order fit to these data.)

The lowest order diagrams which contribute to backward $\pi^+ - p$ scattering are shown in Fig. 5. These diagrams lead to singularities in the unphysical region, $\cos\theta < -1$, and one might expect that the singularity closest to $\cos\theta^* = -1$ is the most important in determining the backward scattering. The neutron-exchange diagram [Fig. 5(a)] can contribute only to $\pi^+ + p$ because of charge conservation; this diagram leads to a pole which is the closest singularity to $\cos\theta^* = -1$. Diagram 5(b) is representative of processes in which a nucleon and one or more pions are exchanged, and these diagrams lead to branch cuts beginning further away from $\cos\theta^* = -1$ than the neutron-exchange pole. If the process represented by Fig. 5(a) is much more important than the processes represented by Fig. 5(b), then one expects the differential cross section to rise in the physical region near $\cos\theta^* = -1$.

Proceeding on this assumption, one can calculate the contribution to backward elastic scattering from the

¹⁰ Our angular distribution at 1.5 BeV/c is in good agreement with that reported by J. A. Helland, T. J. Devlin, D. E. Haggie, M. J. Longo, B. J. Moyer, and C. D. Wood, Lawrence Radiation Laboratory Report UCRL-10263, 1962 (to be published).

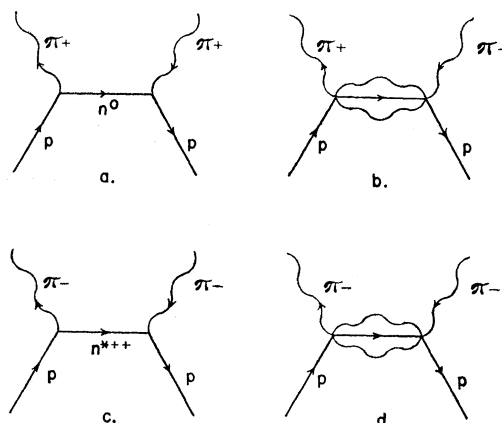


FIG. 5. Diagrams for processes dominating backward scattering.

neutron-exchange pole. If the neutron is an elementary particle, one finds¹¹

$$\begin{aligned} \frac{d\sigma}{d\Omega}(\cos\theta^* = -1)|_{\text{pole}} &= |f_1^{3/2} - f_2^{3/2}|^2 \\ &= \left| \frac{g^2 M}{u - M^2} \left[\frac{(W^2 - M^2 + \mu^2)}{W^2} \right] \right|^2, \end{aligned}$$

where $g^2 \approx 15$, M = nucleon mass, μ = pion mass, W = total energy in the barycentric system, and u is the square of the cross-momentum transfer given by

$$u = M^2 - 2[(q^2 + \mu^2)(q^2 + M^2)]^{1/2} - 2q^2 \cos\theta^* + \mu^2,$$

where q = barycentric momentum. At 2.0-BeV/c incident-pion momentum,

$$\frac{d\sigma}{d\Omega}(\cos\theta^* = -1)|_{\text{pole}} \approx 90 \text{ mb/sr.}$$

Evidently a correct description of $\pi^+ - p$ backward scattering must include the effect of processes represented by Fig. 5(b). Unfortunately, there appears to be no reliable method available for carrying out this calculation within the framework of ordinary dispersion theory.

ACKNOWLEDGMENTS

We wish to thank Denis Keefe, Leroy Kerth, Paul Murphy, William Wenzel, and Theodore Zipf for their generosity in allowing us to use the K^+ apparatus and beam for this experiment, and for their help in taking the data. We also wish to thank Kwan Lai and Clyde Peck for their help in taking the data. Two of us (VC and WRH) wish to thank several LRL theorists, in particular B. M. Udgaonkar and V. Singh, for many illuminating discussions concerning the dispersion-relation analysis. Finally we wish particularly to thank Lawrence Jones for his help, interest, and support throughout the experiment and the analysis.

¹¹ S. C. Frautschi and J. D. Walecka, Phys. Rev. **120**, 1486 (1960).